

Impact on electronic correlations on the structural stability, magnetism, and voltage of LiCoPO₄ battery

O. Le Bacq* and A. Pasturel

Laboratoire de Physique et Modélisation des Milieux Condensés, CNRS, BP 166, 38 042 Grenoble, France

O. Bengone

*Department of Physics, Uppsala University, Box 530, SE-75121, Uppsala, Sweden
and Sweden and Department of Physical Electronic/Photonic, Mitthögskolan, Sundsvall, Sweden*

(Received 21 November 2003; published 17 June 2004)

We present a study of the structural stability of the lithium-orthophosphate oxide LiCoPO₄ using density-functional theory within the local-density (LDA), generalized gradient and LDA+*U* approximation. We show that both enhanced localization and anisotropic effects provided within the LDA+*U* approximation are essential to reproduce the experimentally observed magnetic structure, lattice parameters, and stability of the lithiated and nonlithiated compound. Within this approximation, the intercalation voltage of 4.6 eV as well as the insulator character of the lithiated and nonlithiated compounds are recovered. Moreover, we found that the LDA+*U* approximation induces a strong transfer of charge from the *t*_{2g}-like to the *e*_g-like orbitals of Co as well as a significant shift of the LiPO₄ band. Both effects are competing with each other and determine most of the peculiar properties of the LiCoPO₄ and CoPO₄ compounds.

DOI: 10.1103/PhysRevB.69.245107

PACS number(s): 71.20.Ps, 61.66.Fn

I. INTRODUCTION

The growing demand for safe and environment-friendly portable batteries with high-energy density and low raw materials cost urges for the development of advanced lithium-ion batteries. The performance of such devices depends crucially on the two following factors: (i) reversibility of Li intercalation and Li removal from the host structure which ensures multiple charge and discharge cycles, a compulsory condition for the battery to be reloaded, and (ii) a large value of the free energy of the lithiation-delithiation reaction, directly proportional to the intercalation voltage. Among all the known Li-intercalation compounds, a wide variety of positive active materials, including LiCoO₂, LiNiO₂ (layered structure) (Refs. 1,2) and LiMn₂O₄ (spinel),³⁻⁵ meet these requirements and operate in a voltage range between 3 and 4 Volts, which falls within the voltage range of existing non-aqueous electrolytes.

However, efforts to improve the electrolyte have recently enabled an increase of the potential over 5 V. Among the family of lithium transition-metal orthophosphates within olivinelike structure, efforts were mainly focused on LiFePO₄ operating at 3.5 V.⁶⁻⁸ The Co based compound LiCoPO₄, has rapidly become of particular interest as recent measurements found a potential of 4.8 V,⁹ tractable by the new generation of electrolytes. The works of Amine *et al.*⁹ indicate that lithium can be extracted and intercalated in a reversible way and that the compound keeps its crystal structure during the process. These results suggest a great promise for LiCoPO₄ as cathode material for very high-energy density lithium battery.

The present paper investigates the structural stability, electronic and magnetic structure, as well as the voltage of the LiCoPO₄ oxide using density-functional theory. Our main goal is to determine the microscopic features of LiCoPO₄ which are responsible for its remarkable properties,

and likely to explain in the future the sudden enhancement of the voltage (1 V) for the Co-based olivine host structure.⁹ To this purpose, we examine the required conditions on the CoPO₄ host structure in order to accept Li ions intercalation. We then examine the effects generated by the Li intercalation. In that sense, our procedure is opposite to the experimental one, in which the lithiated compound is always synthesized first and then delithiated. Thus, as a first step, we focus on the nonlithiated compound. We analyze the influence of the electronic correlation effects [choice of local-density approximation (LDA), generalized gradient approximation (GGA), or LDA+*U* approximation] on the structural stability of the compound, its magnetism, and the local environment of Co sites. Both GGA and LDA+*U* approximations represent these properties in a correct way. The LDA approximation leads to a small volume and a nonmagnetic ground state in complete disagreement with the experiments. Indeed, it has been experimentally shown that the lithiated compound displays an antiferromagnetic structure at low temperature.¹⁰ The enhanced localization provided by both the GGA and LDA+*U* approximations compared to LDA were thus found to be a key ingredient of the calculation in order to recover the experimental volume. As a second step, we focus on the lithiated compound for which a similar study is carried out. In addition, we examine the role played by Li and outline its large effect to the stability of the lithiated compound through a full hybridization with the PO₄ band.

Finally, using different approximations, we investigate the impact of electronic correlation effects on the magnitude of the intercalation voltage. Our results show that only the LDA+*U* approximation recovers the experimental results.

II. METHODS

The method of calculation used in the present work is the projector augmented wave (PAW) method^{11,12} as imple-

mented in the Vienna *ab initio* simulation package (VASP) program.¹³ The method, based on the density-functional theory^{14,15} (DFT) is an all-electron method that allowed a correct description of the valence wave functions and its nodal behavior without any shape approximation on the crystal potential. Both spin-polarized DFT calculations and non-collinear magnetism calculations¹⁶ were carried out to investigate the magnetic structure of the oxides. The Vosko, Wilk, and Nusair interpolation¹⁷ for the exchange-correlation potential was used within both the LDA and the GGA. The effects due to the localization of the *d* electrons of the Co ions in the oxide are taken into account within the LDA + *U* approximation as recently implemented in VASP.^{18,19} In the so-called LDA + *U* approximation,²⁰ the spin-polarized LDA potential is supplied by a Hubbard-like term to account for the quasiatomic character of the localized (here Co-3*d*) orbitals. Hence the localized electrons (Co-3*d*) experience a spin- and orbital-dependent potential, while the other orbitals are delocalized and considered to be properly described by the LDA. Although the LDA + *U* is still a mean-field approach, it has the advantage of describing both the chemical bonding and the electron-electron interaction. The corrected functional has the following expression:²¹

$$E_{LDA+U} = E_{LDA} + \frac{U-J}{2} \sum_{\sigma} \text{Tr}[\rho^{\sigma} - \rho^{\sigma} \rho^{\sigma}], \quad (1)$$

where ρ^{σ} is the on-site occupancy matrix, *J* is the screened exchange energy [approximation of the Stoner exchange parameter and almost constant for the 3*d* transition-metal ions = 0.95 eV (Ref. 22)] and $U = E(d^{n+1}) + E(d^{n-1}) - 2E(d^n)$ is the Hubbard parameter, describing the additional energy cost to accommodate an extra electron on a particular site. However, *U* is a renormalized quantity and contains effects due to screening from other types of electrons, e.g., 4*s* and 4*p* from the transition-metal atoms, as well as electrons from the nearest-neighbors atoms, namely oxygen atoms. As a result, additional penalty energies are obtained on the LDA eigenvalues. They correspond to the expected corrections due to the strong one-site Coulomb repulsion of the *d* electrons of the metal in the oxide. The strength of the penalty depends on a single parameter *U* - *J*. The larger the *U* - *J*, the more hybridization effects of the metal with its neighbors is reduced. In fact, for large *U* - *J*, filled *d* orbitals are moved to lower energies by $-(U - J)/2$, and empty *d* orbitals are raised to higher energies by $(U - J)/2$.²¹ The difference *U* - *J* was kept fixed to 4 eV during our calculations as usually met in the literature for a transition-metal oxide.²³ As shown in the following, this value led to reasonable predictions for the different quantities we have investigated.

Numerical integrations in the Brillouin zone were performed by means of the²⁶ tetrahedron method^{27,28} including the Blöchl corrections.²⁹ Sixteen irreducible *k* points were found necessary (for both the 24-atom and 28-atom cells we used) for total energies and magnetic moments of our systems to be converged within 10^{-3} eV and $0.01\mu_B$, respectively.

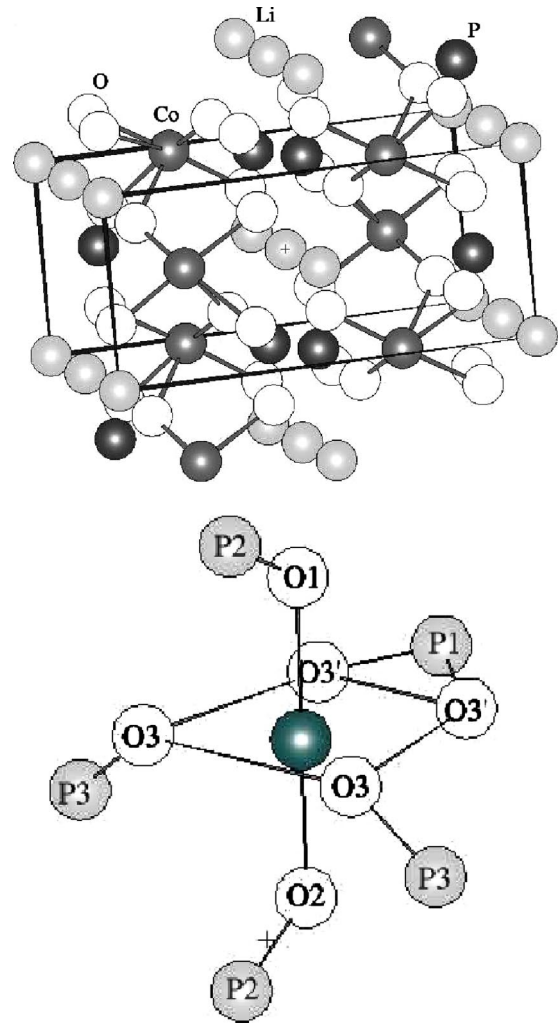


FIG. 1. Olivinelike structure of the LiCoPO_4 compound. Co are enclosed in octahedra of O linked by tetrahedra of O containing the P. The octahedra of O are directly linked to each others by the submits. Rows of Li are intercalated in between. Besides, Co-O-P sequences around a Co ion (darkest atom at the center of the equatorial plane of the octahedra) are represented.

We now turn to a closer description of the oxide we have chosen to study. LiCoPO_4 belongs to a large family of compounds of the $ABPO_4$ type where *A* and *B* stand for monovalent and divalent cations, respectively. These phosphates exhibit different structures depending on the size of the *A* and *B* ions, as for example the arcanite (β - K_2SO_4) (Refs. 30–32) or trydimite (β deformation of SiO_2) (Ref. 33) structure type. For small *A* ions such as Li^+ , the resulting compound, LiCoPO_4 , adopts the olivine (Mg_2SiO_4) (Ref. 34) structure. This structure crystallizes in the orthorhombic system with *Pnma* space group, and consists of a hexagonal close packing of oxygen with Li and *X* ions located in half the octahedral sites and P ions in (1/8)th of the tetrahedral sites.³⁵ In Fig. 1, we present the unit cell (surrounded by few fragments) used in our calculations. The non-lithiated and lithiated compounds contain 24 and 28 atoms in the unit cell, respectively (four additional Li atoms are added in half the octahedral sites). The initial guess for the atomic positions to

TABLE I. The lattice parameters, volume of the cell, magnetic moment of Co ions, and observed deformation of the octahedra of O. NM stands for nonmagnetic and AF for antiferromagnetic.

Composition	Approximation	a (Å)	b (Å)	c (Å)	Ω (Å ³)	$ \mu_{\text{Co}} $ (μ_B)	Deformation of octahedra
CoPO ₄	LDA - NM	9.35	5.33	4.42	220		No
	GGA - NM	9.72	5.57	4.62	250		Weak
	GGA - AF	9.92	5.83	4.75	275	2.75	Yes
	LDA+ U	9.82	5.71	4.64	260	3.03	Yes
	Expt. ^a	10.089	5.855	4.719	279		Yes
LiCoPO ₄	LDA - AF	9.85	5.74	4.59	260	2.38	Yes
	GGA - NM	9.91	5.89	4.71	275		Yes
	GGA - AF	10.24	5.96	4.75	290	2.48	Yes
	LDA+ U	10.02	5.80	4.65	270	2.74	Yes
	Expt. ^a	10.202	5.922	4.699	280		Yes

^aFrom Ref. 9.

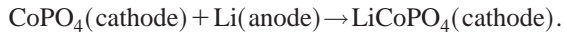
be relaxed were extracted from the experimental x-ray diffraction pattern of polycrystalline LiFePO₄, given in Ref. 10.

To optimize the geometry of the cells, we have performed internal relaxation of the atomic positions for various volumes: using the Hellmann-Feynman theorem, internal coordinates are relaxed so that forces are canceled. We have considered the atomic coordinates as fully relaxed as the size of the individual forces were less than 0.005 eV/Å. A residual minimization method were used for this purpose. The equilibrium properties of the oxides [total energy, lattice parameters, and density of states (DOS)] that we shall discuss in the following, correspond to the ground-state configuration for the atomic and electronic degrees of freedom.

Following previously well established methods,^{36–38} the average intercalation voltage of the battery is given by

$$\bar{V} = -\frac{\Delta G_r}{F}, \quad (2)$$

where F is the Faraday constant, and ΔG_r is the Gibbs free energy for the reaction:



Since the effects due to changes in volume and entropy are small (as easily demonstrated by a simple Debye-Grüneisen approximation for the vibrational energy), the Gibbs energy difference is approximated by the internal energy difference at 0 K (ΔE_r), supplied by our first-principles total-energy calculations through

$$\Delta E_r = E_{\text{LiCoPO}_4} - E_{\text{Li}} - E_{\text{CoPO}_4}. \quad (3)$$

As explained in Ref. 24, the cohesive energy of Li is calculated in the bcc structure which corresponds to the structural phase of the Li anode.

III. NONLITHIATED COMPOUND

A. Lattice parameters and octahedra distortion

In the first panel of Table I, we report the lattice parameters, the equilibrium volume, and the magnetic moment of

Co site in CoPO₄. Nonmagnetic and spin-polarized calculations within the LDA, GGA, and LDA+ U approximations are presented. Our results show that the nonmagnetic calculation within the LDA and GGA approximations drive to a reduced equilibrium volume of 220 Å³ and 250 Å³, respectively, to be compared to the 279 Å³³⁹ experimental value of the lithiated compound. Even if the experimental value,⁹ i.e., 279 Å³, is slightly overestimated since the Li desintercalation is never complete, we can conclude that nonmagnetic calculations underestimate the experimental feature and that the structural stability of the nonlithiated compound is closely connected to its magnetic structure.

Thus the LDA approximation were found unable to generate any magnetism in the compound. On the opposite, both the spin-polarized GGA and LDA+ U approximations induced a stable magnetic structure for the compound (Table I), with magnetic moments on Co sites of 2.75 μ_B and 3.03 μ_B , respectively. Both the approximations lead to an increase of the equilibrium volume, i.e., 275 Å³ (GGA) and 260 Å³ (LDA+ U). To conclude on the structural analysis, we outline that, as these later approximations are used, a noticeable deformation of the octahedra of O surrounding the Co sites is observed. In Fig. 2, we show the difference of charge density between the nonmagnetic LDA and antiferromagnetic LDA+ U approximation for the relaxed atomic positions and equilibrium volume of the LDA+ U approximation. As can be seen, the Co site displays a C_s symmetry: the two “axial” oxygen atoms (O₁ and O₂) are located at 1.90 Å while the four “equatorial” oxygen atoms (O₃) display two different bond lengths, i.e., 1.93 Å (O₃) and 2.14 Å (O₃). Unfortunately the experimental individual atomic coordinates in the CoPO₄ structure are not known and, consequently, we cannot compare directly with our results. Nevertheless, such a deformation of the octahedra were experimentally observed in LiCoPO₄²⁵ with a difference of 0.15 Å between Co—O bonds, in agreement with our calculations. However, let us emphasize that the deformation is not strictly the same in the lithiated and nonlithiated compounds as it will be discussed below.

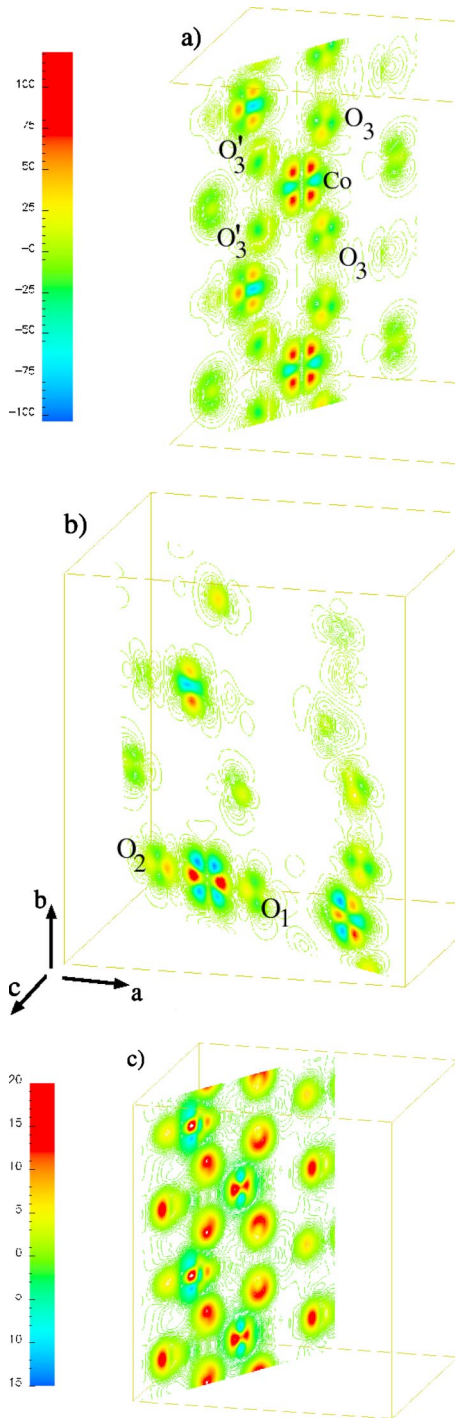


FIG. 2. (Color online) Difference between the charge density of the nonlithiated compound in its antiferromagnetic (LDA+ U) and nonmagnetic (LDA) configuration, $\rho^{+U}(r) - \rho^{LDA}(r)$, in (a) the equatorial plane of the octahedra of O and in (b) a plane containing the vertices of the octahedra. $\rho(r)$ being a positive number, the red region results in a gain of charge for the LDA+ U approximation. In (c), we show the difference between the charge density of the nonlithiated compound calculated within the GGA and LDA+ U approximations, i.e., $\rho^{GGA}(r) - \rho^{+U}(r)$. Additional charge is obtained on the sites of oxygen within the GGA.

The influence of the exchange interaction on the intercalation voltage may be calculated by the energy difference of the antiferromagnetic and ferromagnetic configuration, i.e.,

$$J^{xc} = E_{tot}(\downarrow\uparrow) - E_{tot}(\uparrow\uparrow), \quad (4)$$

where $E_{tot}(\downarrow\uparrow)$ is the total energy of the compound in an antiferromagnetic configuration and $E_{tot}(\uparrow\uparrow)$ is the total energy in a ferromagnetic one. This energy difference does not exceed 0.02 eV/atom, leading to negligible corrections to the Li intercalation voltage. In addition, we have performed a noncollinear magnetism calculation for LiCoPO₄ while polarizing the total magnetic moment along three different crystallographic directions, i.e., [001], [010], and [100]. We obtained a 0.03 eV stabilization energy (with respect to the collinear case) for magnetic moments pointing along the $\mathbf{a} = [001]$ axis. A fine analysis of the noncollinear magnetic structure of the compound (not represented) shows that the magnetization was strongly focused on the Co ions, non-tilted, and was presenting a very regular alignment of the moments along the same axis, legitimating the use of collinear magnetism calculations for our study.

B. Electronic structure

The interesting question we would like to address here is the determination of the critical character in common with the GGA and LDA+ U approximation which allows to obtain a better equilibrium volume, magnetic structure, as well as a realistic description of the local environment around Co sites. Figure 2 supplies the answer: the antiferromagnetic LDA+ U approximation (or the GGA not shown) gives a charge transfer (with respect to the nonmagnetic LDA description) from the t_{2g} orbitals, pointing in between the O sites to the e_g orbitals, pointing towards the O sites. This implies larger electronic repulsions between Co and the O octahedra. As a consequence, the bond length between Co and O sites tends to be larger and the total equilibrium volume of the cell is thus increased as the octahedra is swelled by electrostatic repulsion effects. Another consequence is to break the symmetry of Co sites, namely the deformation of the equatorial plane of the octahedra, which induces a local moment on Co atoms. This results from the additional charge-density anisotropy provided by orbital polarization effects and gradient corrections within LDA+ U and GGA, respectively. The LDA, relying on the theory of the homogeneous electron gas, may not introduce this anisotropic character, and fails to recover the characteristics of the oxide.

The analysis of the projected densities of states on Co confirms this explanation. They are presented in Figs. 3(a) and 3(b). Within the LDA, the d_{xy} , d_{yz} , and d_{xz} orbitals (presenting a t_{2g} character) contain most of the d electrons, while the d_{z^2} and $d_{x^2-y^2}$ orbitals (e_g character) contain a negligible fraction of them. Spin-up and spin-down bands are filled equally and magnetism is killed. Therefore, we may consider that, within the LDA, the system presents a large similarity in behavior with systems driven by crystal-field effects with a low spin configuration.

The striking difference between LDA and LDA+ U calculations is the antiferromagnetic character of the compound

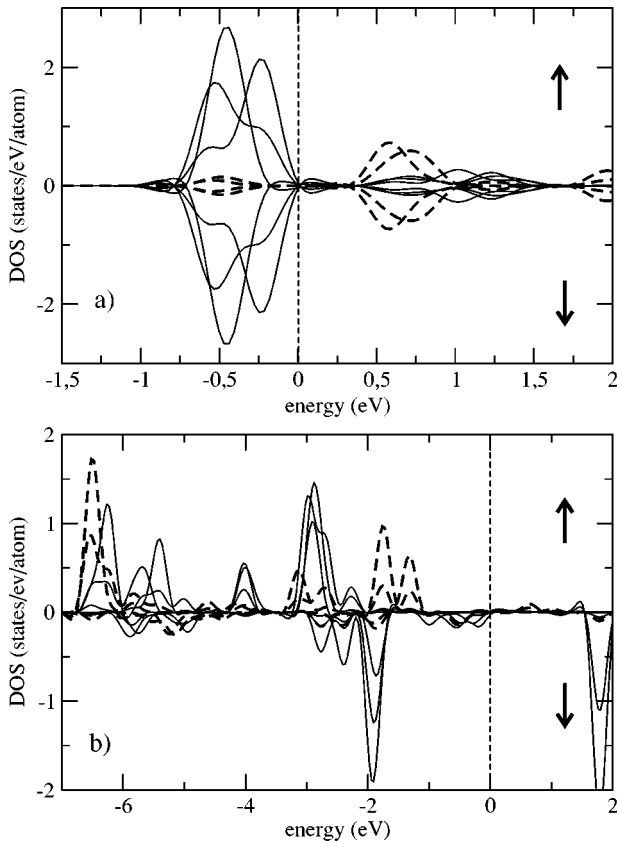


FIG. 3. d_{xy} , d_{xz} , d_{yz} , $d_{x^2-y^2}$, and d_{z^2} projected densities of states of the Co site in CoPO_4 within (a) the nonmagnetic LDA and (b) the antiferromagnetic LDA+ U approximations. An e_g character is attributed to the $d_{x^2-y^2}$ and d_{z^2} orbitals (dashed lines) and a t_{2g} character to the d_{xy} , d_{xz} , and d_{yz} orbitals (solid lines). The Fermi energy is represented by a vertical line.

with a magnetic moment of $3.03 \mu_B$ on cobalt. The exchange splitting found in the LDA+ U leads to important difference between density of states of Co calculated either by LDA or LDA+ U (see Figs. 3 and 4).

The simple view given by LDA, i.e., all the t_{2g} orbitals are empty, does not hold within LDA+ U (or GGA) calculations. In the latter ones, the partial DOS of Co can be under-

stood from partial spin-up and spin-down DOS, both having the sequence t_{2g} and e_g bands. Consequently, spin-up electrons occupy t_{2g} -like orbitals only partially (conservation of the total charge).

Figures 4(a)–4(c) display the site-projected density of states on Co sites and Figs. 4(d)–4(f) on the PO_4 fragment, calculated within the LDA, GGA, and LDA+ U . For all the approximations, a wide and fully hybridized band is obtained for the PO_4 fragment [Figs. 4(d)–4(f)]. This latter spreads out from the Fermi energy to -8 eV within the LDA+ U and GGA approximations. Within LDA+ U and GGA approximations, the PO_4 band presents very few similarities in shape with the Co band so that we may conclude that the PO_4 band hybridizes very weakly with the Co band. As previously mentioned, this is a consequence of the different orbital polarization of the Co- d electrons within the LDA+ U approximation, introducing an anisotropy in the charge density. The same behavior holds for the GGA for which the anisotropy is obtained by the introduction of the gradient of the charge density in the exchange and correlation potential.

C. Spin transfer mechanism

Thus, the electronic structure of our system (within the LDA+ U) may not be considered as ruled out any more by crystal field-effects but by the competition between polarization and delocalization effects as recently introduced by Carlier *et al.*³⁹ In the present study, these effects should result in the possible overlapping of Co, O, and P orbitals to form a spin orbital in the crystal if a particular symmetry that we shall discuss in the following is present (delocalization) or in a polarization effect due to the unpaired electrons of the Co orbitals, which polarize all the other surrounding doubly occupied spin orbitals (polarization). This latter phenomenon is directly related to the fact that electrons with the same spin as the unpaired electrons of Co spend more time near Co than electrons with opposite sign. This is a consequence of the exchange interaction. As a result, positive spin density on Co is enhanced while negative spin density is induced on the p orbitals of O and P, leading to a resulting negative charge on P. The analysis of the interaction geometry (symmetry and orientation of the orbitals involved in the Co-O-P sequence)

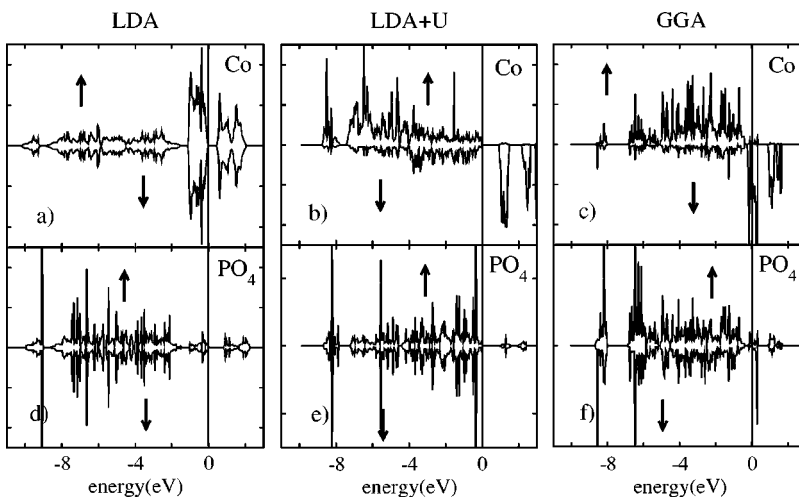


FIG. 4. Density of states of Co ion in CoPO_4 within (a) LDA, (b) LDA+ U , and (c) GGA approximation. In the bottom panel, density of states of the phosphate fragment (PO_4) in CoPO_4 calculated within (d) LDA, (e) LDA+ U , and (f) GGA are added. The Fermi energy is represented by a vertical line.

has to be considered to determine the dominant mechanism. In CoPO_4 , two types of Co-O-P sequence have to be distinguished which are as follows.

(i) The $\text{Co-O}_2\text{-P}_2$ or $\text{Co-O}_1\text{-P}_2$ sequences are both located in the same plane (see Fig. 1) with distances of $d_{\text{Co-O}} = 2.1 \text{ \AA}$ and $d_{\text{P-O}} = 1.5 \text{ \AA}$, and an angle of 120 deg.

(ii) The $\text{Co-O}_3\text{-P}$ sequence is split into two subgroups. The first one, $\text{Co-O}'_3\text{-P}_1$, involving the O'_3 sites, belongs to the equatorial plane of the octahedra with an angle of 94 deg. The second contains O_3 sites and P_3 sites with angles of 124 deg; let us mention that P_3 sites belong to an orthogonal plane to the equatorial plane.

Thus, five different Co-O-P sequences participate in the mechanism of polarization or localization on P sites. The analysis of the projected charge in the augmentation spheres centered on P sites may help us to determine which one predominates. Our calculations actually predict two additional electrons on P site, leading to a resulting negative charge expected by the polarization mechanism. From this, we can conclude that the polarization mechanism dominates and that a spin transfer occurs throughout the e_g orbitals containing a single electron (as confirmed by integrating the DOS of the d_{z^2} orbital, given on Fig. 3) and the p orbitals of O and P atoms. The analysis of the spin density mapped in the plane containing both the $\text{Co-O}_2\text{-P}$ and $\text{Co-O}_1\text{-P}$ sequences (not represented) confirms this mechanism: a positive spin density is observed in the e_g orbital of Co, pointing towards O_2 and O_1 , polarizing the paired electrons in the p orbitals of P and O (no magnetism is induced on these sites).

D. Comparison between LDA+ U and GGA approximations

To conclude our results for the nonlithiated compound, we would like to emphasize the major discrepancies between the GGA and LDA+ U approximations. Figures 4(b) and 4(c) display a comparison between the site-projected density of states of Co ion in CoPO_4 using the two approximations. We observe that a half-metal character is obtained within the GGA, whereas an insulator one is recovered within the LDA+ U , in agreement with the experiments.⁴⁰ Although the polarization effects within the GGA allow an occupancy in the e_g -like and t_{2g} -like orbitals responsible for the magnetism and the larger volume of the oxygens octahedra, these effects remain insufficient. In particular, a peak with e_g character is still observed at the Fermi level, leading to the half-metal character.

In Fig. 2(c), we display the difference of charge density calculated within the GGA and LDA+ U approximations. The results show that the GGA brings additional charge on the O sites (with respect to the LDA+ U calculation) and redistribute the internal charge on Co sites. This redistribution consists in a larger occupancy in the t_{2g} orbitals and a less important one in the e_g orbitals within the GGA than within the LDA+ U . Nevertheless, the occupancy in the e_g orbitals remains pronounced compared to the LDA and nonmagnetic calculations. The main improvement of both these approximations compared to the LDA is a better description of the anisotropy of the charge density (although anisotropy is generated differently within both the approximations).

The repulsion effects between the excess electrons (within the GGA) from the equatorial oxygen atoms of the deformed octahedra O_3 and O'_3 of Fig. 1, contribute to enhance Co-O bond lengths compared to the LDA+ U approximation (see volumes in Table I). We nevertheless argue that these additional electronic repulsions inherent to the GGA approximation remains artificial and does fail to recover the expected electronic structure of the CoPO_4 compound. Note that our remark specifically concerns this peculiar compound and that the GGA was found in the past to be suitable to represent the electronic structure of numerous other oxides.³⁶

IV. LITHIATED COMPOUND

Most of the characteristics (structural and electronic structure) of the lithiated compound are similar to the ones of the nonlithiated compound. For this reason, the results of the present section will mainly outline the additional effects we have acquired with respect to the nonlithiated compound as Li is intercalated.

A. Structural properties

Structural parameters of LiCoPO_4 are given in Table I and compared to the experiments. Nonmagnetic LDA calculations were found unable to describe the characteristics of the oxide. Only the AF-GGA (AF, antiferromagnetic) and LDA+ U are in good agreement with the experiments, with an acceptable mechanical resistance along the b axis and a correct symmetry for Co site. Note that for all approximations, the intercalation of Li leads to a larger volume (about 5%) with respect to the nonlithiated compound.

The deformation in the equatorial plane is similar to the one found in the nonlithiated compound, corresponding to a splitting into two shells with bond lengths of 2.01 and 2.14 \AA .³ Nevertheless, contrary to the CoPO_4 case, axial oxygen atoms (O_1 and O_2) do not present the same distance with respect to the Co site with $d_{\text{Co-O}_1} = 2.12 \text{ \AA}$ and $d_{\text{Co-O}_2} = 2.01 \text{ \AA}$. This may be explained by the inequivalent response of the two types of oxygen (O_1 and O_2) as lithium is intercalated in only half the tetrahedral sites of the host-structure (if all the tetrahedral sites were empty, O_1 and O_2 should be equivalent).

B. Electronic structure

For the lithiated compound calculated within LDA+ U , we use the same $U-J$ value of 4 eV as for the nonlithiated compound. As mentioned previously, the effective Coulomb energy U is an on-site quantity, although renormalized due to screening. As Li atoms do not belong to the nearest-neighbor shell of Co atoms, the value of U should not change significantly as Li atoms are inserted.

The analysis of the difference of charge densities calculated within the LDA and LDA+ U approximations (not represented) shows that the charge transfer from the t_{2g} to the e_g orbitals is similar to the one obtained in CoPO_4 . A difference is nevertheless observed compared to the nonlithiated compound: within both the approximations (LDA and LDA

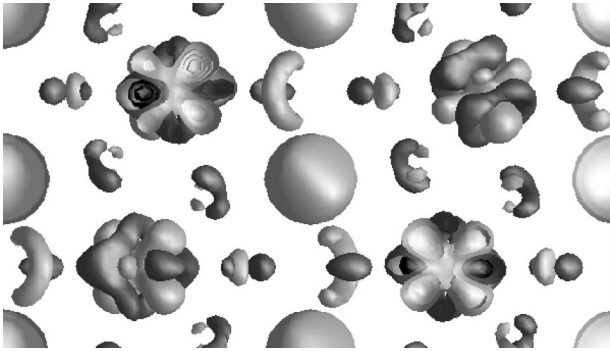


FIG. 5. Top view of the difference of charge density (DCD) between LiCoPO_4 and CoPO_4 . Dark regions represent a gain of charge for the lithiated compound. Two DCD's of Co are seen in cut, two of them, deeper in the cell, display the peculiar entanglement of excess and lacking electrons regions on Co in LiCoPO_4 (compared to CoPO_4). Excess electrons are found in the e_g orbitals pointing towards the oxygen atoms, located all around. The row of spherical charge densities in the center corresponds to the row of intercalated Li ions.

+ U), the occupancy in the e_g orbital is larger for the lithiated compound than for the nonlithiated (see Fig. 5). This explains the larger volume, even within the LDA. Moreover, contrary to CoPO_4 , we found that the lithiated compound is magnetic within the LDA. This better description within the LDA for LiCoPO_4 than for CoPO_4 , may be explained by the introduction of an anisotropic character in the charge density as Li is intercalated in only half the tetrahedral sites (O_1 and O_2 are not equivalent anymore). However, a comparison of the Co site-projected charge in the augmentation sphere in LiCoPO_4 and CoPO_4 shows that this internal redistribution of charge on Co sites does not imply a change of the total

charge of Co: the additional electrons obtained in the e_g orbitals are transferred from the t_{2g} ones. Thus, no change of the valence state is observed within our approximations, although our analysis of the electron and spin populations does not allow to define metal cations with formal charges as in the classical view of solid-state materials. The appearance of magnetism within the LDA seems to only result from the internal redistribution of charge on Co (anisotropy) and from the larger equilibrium volume. The fact that no change in the valence of Co is present is not surprising as the physics of LiCoPO_4 is not piloted by the crystal-field effects which should impose it.

The calculated resulting charge on P site in LiCoPO_4 is negative with 1.7 excess electrons compared to 2 excess electrons in the nonlithiated compound. As Li is intercalated in half the tetrahedral sites of the host structure, the oxygen sites, involved in the polarization mechanism with P, have to share a new bonding with Li, creating an additional pathway of polarization. As a result, polarization effects on P are lowered while a polarization effect is developed on Li. The internal redistribution of charge in Co (with respect to the nonlithiated compound) is a consequence of this new polarization effect involving a different set of orbitals than the one involved in the Co-O-P sequence. This spin transfer mechanism gives rise to the observed magnetism and leads to a net spin moment of $2.75\mu_B$ (see Table I) on the Co sites, slightly less, compared to the nonlithiated case.

Figure 6 shows the site-projected densities of state in LiCoPO_4 calculated within the three approximations. Within the three approximations, we observe that, as Li is intercalated into the CoPO_4 host structure, the Li band fully hybridizes with the phosphate PO_4 band [Figs. 6(d)–6(i)]. The LDA and GGA approximations lead to similar DOS. Within these approximations, the hybridization of the Li states with

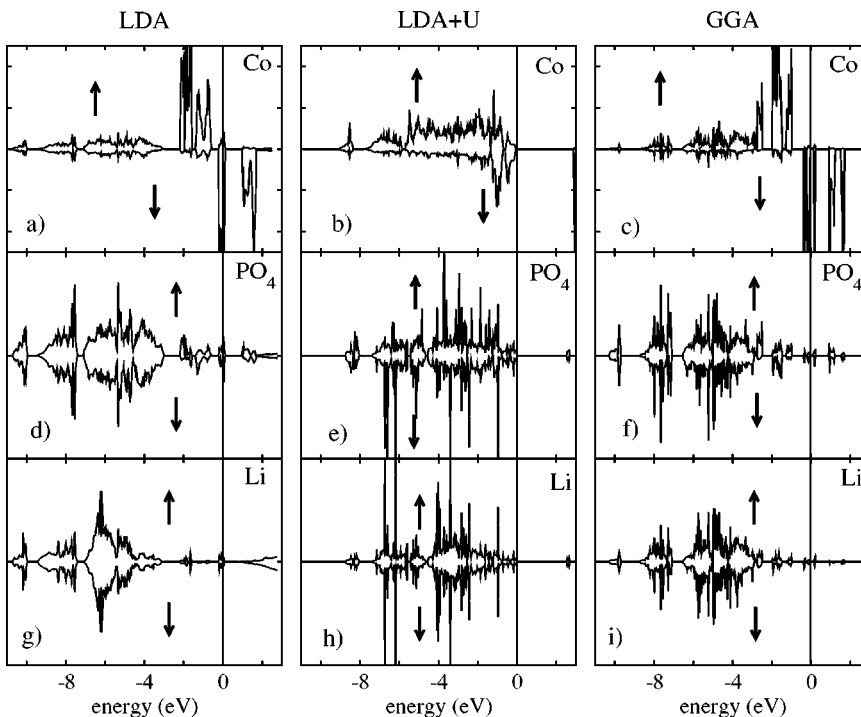


FIG. 6. Density of states of Co ion in LiCoPO_4 within (a) LDA, (b) LDA+ U , and (c) GGA approximation. Second row [(d)–(f)], presents the site-projected DOS on the phosphate fragment (PO_4) and the third row [(g)–(i)] the site-projected DOS on Li site. The Fermi energy is represented by a vertical line.

TABLE II. Calculated total energies of the nonlithiated and lithiated compounds and intercalation voltage of the battery.

	LDA			GGA		Expt.
	NM	AF	+ U	NM	AF	
E_{CoPO_4} (eV)	-187.70	idem NM	-178.45	-166.80	-166.83	
E_{LiCoPO_4} (eV)	-207.41	-208.71	-205.00	-185.85	-188.95	
Voltage (V)	2.90	3.20	4.60	2.87	3.64	4.80

^aFrom Ref. 9.

the PO_4 band is mainly observed around -5 eV and -8 eV, i.e., far from the Fermi energy, where the metallic peaks are mainly observed. Two main peaks may be distinguished: a first one (the closest to the Fermi energy) with an e_g character and the second with a t_{2g} character. As already observed on the charge density map, e_g and t_{2g} bands are filled more equally than in the case of the nonlithiated compound due to internal charge redistribution.

As for the nonlithiated compound, the LDA+ U approximation leads to the formation of a wide Co-band formed with e_g and t_{2g} -like bands, spreading out from -8 eV to the Fermi energy. The translation of both the partially filled e_g and t_{2g} -like bands by an amount of $-(U-J)/2$ leads to the expected insulator character for the oxide. However, the most important point to note is that the formation of such a wide Co band affects the LiPO_4 band, since both its shape and its location with respect to the Fermi energy are changed with respect to both the other approximations. Such a change was clearly observed in the nonlithiated compound.

V. INTERCALATION VOLTAGE

Total energies of the lithiated and nonlithiated compounds as well as the voltage obtained within the nonmagnetic and magnetic LDA, LDA+ U , and GGA approximations are given in Table II. Our results show that these data are strongly influenced by the magnetic configuration of the compound and the approximation used for the exchange-correlation potential. We note from the first line of Table II that the magnetic structure does not affect the total energy of the nonlithiated compound: both spin-polarized and non-spin-polarized GGA calculations lead to -166.8 eV for the 24-atom cell. On the opposite, the magnetic structure of LiCoPO_4 brings -1.3 eV and -3.1 eV, within the LDA and GGA, respectively, to the total energy of the 28-atom cell, stabilizing the compound. The better ability of the GGA approximation to represent the electronic correlations in Co than the LDA, and thus to represent the octahedral distortion in the structure, may explain this larger stabilization energy in LiCoPO_4 as a spin-polarized calculation is considered. However, as these effects are underestimated by the GGA, such an approximation fails to give a reasonable value for the intercalation voltage, with an underestimation of 1.2 eV with respect to the experiments.

The treatment of the electronic correlation by a LDA+ U scheme consists, in our study, in a destabilization of the structure by filling e_g states (addition of a penalty energy on the eigenvalues). This was found possible by emptying one

spin channel over two, generating magnetism. This destabilization energy is seen to be larger for the nonlithiated compound, $+9.3$ eV, than for the lithiated compound, $+2.4$ eV, leading by difference to a voltage of 4.6 V, in good agreement with the experiments. This asymmetrical energetic response of LiCoPO_4 and CoPO_4 may be explained by the competition between two effects as follows.

(i) First, by the asymmetrical occupancy in the e_g and t_{2g} d orbitals of Co: as the partially filled e_g band is translated by an amount of $-(U-J)/2$ (more e_g states are thus occupied), changes are less important in compounds already having a large occupancy in the e_g 's (as LiCoPO_4) than in compounds having less occupied e_g orbitals (as CoPO_4) which need to modify their electronic structure in a deeper manner. In CoPO_4 , the large peaks of Co near the Fermi energy (E_F), observed within the LDA [Fig. 4(a)], are partially recovered at the bottom of the band within the LDA+ U [Fig. 4(b)], while in LiCoPO_4 [Figs. 6(a) and 6(b)] a large part of these peaks (LDA) remains close to the Fermi energy within the LDA+ U . The change in band energy for Co (negative number since $E_F=0$) is thus larger for CoPO_4 than for LiCoPO_4 as we switch from LDA to LDA+ U .

(ii) Second, by the displacement of the $(\text{Li})\text{PO}_4$ band as the LDA+ U is used or not. The translation of the $(\text{Li})\text{PO}_4$ band towards the Fermi energy brings a positive energy to the compound. This effect was found more important for the lithiated compound, emphasizing the role of the Li ions in the shape and the center of the band.

We easily understand from this, that these two contributions mostly compensate each other in LiCoPO_4 (so that the total destabilization energy is 2.4 eV), whereas the very weak displacement of the PO_4 band in CoPO_4 as the LDA+ U approximation is used, does not compensate the deep change of the Co band (the total destabilization energy is found to be 9.3 eV)

To conclude let us emphasize that the interplay between both contributions is expected to strongly depend on the transition-metal ion, and thus likely to explain the major difference between the voltages of the Co- and Fe-based compounds.

VI. CONCLUSIONS

Ab initio calculations were performed to shed light on the microscopic origin of the peculiar properties of the LiCoPO_4 battery. Three different exchange and correlation potentials

(LDA, GGA, and LDA+ U) were used for this purpose. Our results show that only the LDA+ U approximation is able to provide reasonable predictions for the crystallographic, magnetic, and electronic structures and voltage of CoPO₄ and LiCoPO₄ compounds. The comparison of the three approximations has nevertheless allowed to emphasize the role played by the Co- d orbitals on the previously quoted properties as well as the influence of the anisotropy of the charge density, obtained by different orbital polarizations of the Co- d electrons within the LDA+ U or with the introduction of the gradient corrections within the GGA.

More specifically, we have shown that the LDA+ U gives a physical filling of the e_g d orbitals of Co for both the lithiated and nonlithiated compounds. This is made possible by taking into account spin-polarization effects which translates some e_g states of a given spin channel below t_{2g} states of the other spin channel. The filling of the e_g orbitals introduces additional repulsion effects between the d electrons of Co and the p electrons of the octahedra of oxygen containing Co, so that bond lengths are increased with respect to the nonmagnetic LDA calculation.

The main consequence of the intercalation of Li ions in half the tetrahedral sites of CoPO₄ lies in a larger anisotropy in the charge density of the compound, and, consequently, in the modification of the polarization mechanism, driving to an internal redistribution of charge density in the e_g and t_{2g} orbitals of Co. The ability (or not) of Li to modify the shape

of the LiPO₄ band, according to the treatment of the electronic correlation effects, were found essential to explain the discrepancies between the total energy of the lithiated compound within the LDA, GGA, and LDA+ U approximations. Moreover, this latter effect outlines the deep contribution of Li in the cohesion of the lithiated compound.

These points were found crucial to explain the asymmetrical energetic response of both the compounds as a $U-J=4$ eV Hubbard parameter is used. The additional energy cost provided by the LDA+ U approximation is found adequate to compensate the lack in energy of the LDA approximation and finally we obtain a calculated voltage of 4.6 eV to be compared to the experimental 4.8 eV.

As a prospect to this paper, a systematic study of the LiXPO₄ series, where $X=Mn, Fe, Co,$ and Ni is undertaken in order to understand the sudden enhancement of the voltage of the Co-based compound with respect to the Fe based.

ACKNOWLEDGMENTS

Most of the computations presented in this paper were performed on the cluster PHYNUM (CIMENT, Grenoble), the remaining on the Brodie cluster (IDRIS) as part of the Project No. 21508. A. M. Dulac and S. Jobic are acknowledged for early discussions concerning this work. One of the authors, O.B. is grateful to the Swedish Research Council (VR) and to the Göran Gustafsson foundation for support.

*Electronic address: olivier.lebacq@grenoble.cnrs.fr

¹K. Mizushima, P.C. Jones, P.J. Wiseman, and J.B. Goodenough, *Mater. Res. Bull.* **15**, 783 (1980).

²M.G. Thomas, W.I. David, and J.B. Goodenough, *J. Electrochem. Soc.* **20**, 1137 (1985).

³M.M. Thackeray, P.J. Johnson, L.A. De Picciotto, P. G Bruce, and J.B. Goodenough, *Mater. Res. Bull.* **19**, 179 (1984).

⁴T. Ohzuku, M. Kitagawa, and T. Hirai, *J. Electrochem. Soc.* **137**, 769 (1990).

⁵J.M. Tarascon and D. Guymard, *Electrochim. Acta* **38**, 1221 (1993).

⁶A.S. Andersson, B. Kalska, L. Häggström, and J.O. Thomas, *Solid State Ionics* **130**, 41 (2000).

⁷A. Yamada, S.C. Chung, and K. Hinokuma, *J. Electrochem. Soc.* **148**, A224 (2001).

⁸M. Takahashi, S. Tobishima, K. Takei, and Y. Sakurai, *J. Power Sources* **97-98**, 508 (2001).

⁹K. Amine, H. Yasuda, and M. Yamachi, *Electrochem. Solid-State Lett.* **3**, 178 (2000).

¹⁰R.P. Santoro and R.E. Newnham, *Acta Crystallogr.* **22**, 344 (1967).

¹¹P.E. Blöchl, *Phys. Rev. B* **50**, 17 953 (1994).

¹²G. Kresse and D. Joubert, *Phys. Rev. B* **59**, 1758 (1999).

¹³G. Kresse and J. Hafner, *Phys. Rev. B* **47**, RC558 (1993); G. Kresse, Ph.D. Thesis, Technische Universität Wien, 1993; G. Kresse and J. Furthmüller, *Phys. Rev. B* **54**, 11 169 (1996).

¹⁴P. Hohenberg and W. Kohn, *Phys. Rev.* **136**, B864 (1964).

¹⁵W. Kohn and L.J. Sham, *Phys. Rev.* **140**, A1133 (1965).

¹⁶D. Hobbs, G. Kresse, and J. Hafner, *Phys. Rev. B* **62**, 11 556 (2000).

¹⁷S.H. Vosko, L. Wilk, and M. Nusair, *Can. J. Phys.* **58**, 1200 (1980).

¹⁸A. Rohrbach, J. Hafner, and G. Kresse, *J. Phys.: Condens. Matter* **15**, 979 (2003).

¹⁹O. Bengone, M. Alouani, P. Blöchl, and J. Hugel, *Phys. Rev. B* **62**, 16 392 (2000).

²⁰V.I. Anisimov, J. Zaanen, and O.K. Andersen, *Phys. Rev. B* **44**, 943 (1991).

²¹S.L. Dudarev, G.A. Botton, S.Y. Savrasov, C.J. Humphreys, and A.P. Sutton, *Phys. Rev. B* **57**, 1505 (1998).

²²I.V. Solovyev, P.H. Dederichs, and V.I. Anisimov, *Phys. Rev. B* **50**, 16 861 (1994).

²³F.M.F. de Groot, J.C. Fuggle, B.T. Thole, and G.A. Sawatzky, *Phys. Rev. B* **42**, 5459 (1990).

²⁴S.K. Mishra and G. Ceder, *Phys. Rev. B* **59**, 6120 (1999).

²⁵A. Goñi, L. Lezama, G.E. Barberis, J.L. Pizarro, M.I. Arriortua, and T. Rojo, *J. Magn. Magn. Mater.* **164**, 251 (1996).

²⁶O. Garcia-Moreno, M. Alvarez-Vega, F. Garcia-Alvarado, J. Garcia-Jaca, J.M. Gallardo-Amores, M.L. Sanjuan, and U. Amador, *Chem. Mater.* **13**, 1570 (2001).

²⁷O. Jepsen and O.K. Andersen, *Solid State Commun.* **9**, 1763 (1971).

²⁸G. Lehmann and M. Taut, *Phys. Status Solidi B* **54**, 469 (1972).

²⁹P.E. Blöchl, O. Jepsen, and O.K. Andersen, *Phys. Rev. B* **49**, 16 223 (1994).

³⁰M. Ben Amara, M. Vlasse, G. Le Flem, and P. Hagenmuller, *Acta Crystallogr., Sect. C: Cryst. Struct. Commun.* **39**, 1483 (1983).

³¹A.W. Kolsi, M. Quarton, and W. Freundlich, *J. Solid State Chem.* **36**, 107 (1981).

- ³²C.W. Struck and J.G. White, *Acta Crystallogr.* **15**, 290 (1962).
- ³³L. Elammari and B. Elouadi, *J. Chem. Phys.* **88**, 1969 (1991).
- ³⁴H. D. Megaw, *Crystal Structures: A Working Approach* (W. B. Saunders, London, 1973), p. 249.
- ³⁵S. Geller and J.L. Durand, *Acta Crystallogr.* **13**, 325 (1960).
- ³⁶G. Ceder, M.K. Aydinol, and A.F. Kohan, *Comput. Mater. Sci.* **8**, 161 (1997).
- ³⁷M.K. Aydinol and G. Ceder, *J. Electrochem. Soc.* **144**, 3832 (1997).
- ³⁸M.K. Aydinol, A.F. Kohan, G. Ceder, K. Cho, and J. Joannopoulos, *Phys. Rev. B* **56**, 1354 (1997).
- ³⁹D. Carlier, M. Ménétrier, C.P. Grey, C. Delmas, and G. Ceder, *Phys. Rev. B* **67**, 174103 (2003).
- ⁴⁰A. M. Dulac, Ph.D. thesis, University of Nantes, 2002.